





Magnetic and structural entropy contributions to the multicaloric effects in Ni-Mn-Ga-CuAdrià Gràcia-Condal ^{*}, Antoni Planes , and Lluís Mañosa [†]*Departament de Física de la Matèria Condensada. Facultat de Física. Universitat de Barcelona. Martí i Franquès, 1. 08028 Barcelona. Catalonia*Zhiyang Wei ^{*} and Jianping Guo*Ningbo Institute of Materials Technology and Engineering, Chinese Academy of Sciences, Ningbo 315201, China*Daniel Soto-Parra *Tecnológico Nacional de México. Instituto Tecnológico de Delicias. Paseo Tecnológico, km. 3.5, Cd. Delicias, Chihuahua, CP. 33000. Mexico*Jian Liu [‡]*Center for Advanced Solidification Technology, School of Materials Science and Engineering, Shanghai University, Shanghai 200444, China*

(Received 4 May 2022; accepted 18 July 2022; published 3 August 2022)

We have studied the multicaloric properties of a Ni-Mn-Ga-Cu alloy. In this alloy, application of magnetic field and uniaxial stress shift its martensitic transition towards higher temperatures which results in synergic magnetocaloric and elastocaloric effects. By a proper numerical treatment of the calorimetric curves obtained under applied magnetic field and uniaxial stress we have obtained the entropy $S(T, \mu_0 H, \sigma)$ as a function of the magnetic field, uniaxial stress, and temperature over the whole phase space under study. We have determined the different entropy contributions to the multicaloric effect in this alloy, and noticeably we have evidenced the role played by the interplay between magnetic and vibrational degrees of freedom. A comparison between single caloric and multicaloric effects shows that appropriate combinations of magnetic field and stress reduce the magnitude of the specific field required to obtain a given value of the isothermal entropy and adiabatic temperature changes. For example, at 299 K, to achieve an entropy change (ΔS) of $-14 \text{ J kg}^{-1} \text{ K}^{-1}$, a magnetic field of $\sim 2.5 \text{ T}$ or a uniaxial stress of 19 MPa are required, while a combination of dual fields of (1 T, 12 MPa) yields to the same value of ΔS . Moreover, the maximum adiabatic temperature change is enlarged up to 9.4 K by the dual fields, higher than the value obtained by a single field ($\sim 7 \text{ K}$). The advantage of multicaloric effect is particularly relevant at low magnetic fields which are achievable by permanent magnets. Our findings open new avenues for using multicaloric materials in novel refrigeration technologies.

DOI: [10.1103/PhysRevMaterials.6.084403](https://doi.org/10.1103/PhysRevMaterials.6.084403)**I. INTRODUCTION**

Solid state refrigeration relying on caloric effects in solids is acknowledged as the most promising technology to replace the current vapor compression based refrigeration thanks to its high efficiency and extremely low greenhouse effect potential value [1]. Caloric effects are quantified by isothermal entropy (ΔS) and adiabatic temperature (ΔT) changes, which are induced by application and removal of external field(s) including magnetic field [2] (magnetocaloric effect), electric field [3] (electrocaloric effect), uniaxial stress [4,5] (elastocaloric effect), and hydrostatic pressure [6] (barocaloric effect).

Materials with large caloric effects, associated with a first-order phase transition, have been discovered in the past two decades [7–11], and the recent emergence of a series of

materials with colossal caloric effects has further fueled the research on this topic. Among them, colossal barocaloric effect in plastic crystals with isothermal entropy changes in the range 300–500 $\text{J kg}^{-1} \text{ K}^{-1}$ have been reported [12–14]. Another family of promising caloric materials are spin-crossover complexes, in which huge [15] and reversible [16] barocaloric effects were achieved. In addition to these barocaloric materials, encouraging elastocaloric materials have also been discovered, such as all-*d*-metal Heusler alloys [17,18]. This kind of new alloys show improved mechanical properties (breaking strength $> 1.2 \text{ GPa}$) [19] and large latent heat (up to 76 $\text{J kg}^{-1} \text{ K}^{-1}$) conferring them a significant barocaloric effect [20,21] and an outstanding elastocaloric effect [22–24].

While improving the absolute value of ΔS and ΔT [7] is a requisite for potential use of the materials in applications, there are also other parameters which also play a relevant role because they determine the energy efficiency and cyclability of a caloric material [25–27]. These are hysteresis effects and a lower field to induce the phase transition (critical field). Various strategies including tailoring lattice compatibility between parent phase and product phase [28], texture

^{*}These authors contributed equally to this work.[†]lluís.manosa@fmc.ub.edu[‡]liujian@shu.edu.cn

control [29], second-phase introduction [30], and additive manufacturing [31] were adopted to reduce hysteresis and to lower the critical field. For those materials with coupling between different degrees of freedom, application of more than one type of external field provides a strategy for controlling hysteresis [32] and/or lowering the critical fields [33].

The simultaneous or sequential change of more than one external field gives rise to the so-called multicaloric effects [34]. The thermodynamic framework of multicaloric effects is well established [35], but its experimental study is just at the beginning [36–39]. Materials that can be triggered by either a magnetic field or a mechanical field, or combination of the two fields, are the focus of interest in multicaloric effect research [40]. It was reported that, for Fe-Rh, applying pressure and magnetic field properly enables control of the sign of the entropy change, and expands the temperature window for multicaloric [37] effects. Recently, it was shown that in Ni-Mn-In the multicaloric isothermal entropy change resulting from the combined action of a 1 T magnetic field and a 40 MPa uniaxial stress was significantly larger than the value resulting from a single stimulus [33]. Furthermore, a hydrostatic pressure of ~ 1 GPa was found to be able to enhance the magnetocaloric effect by 8% in Ni-Mn-In alloys [41].

The study of multicaloric effects has mainly been conducted on materials with inverse magnetocaloric effect and conventional mechanocaloric effects. In these materials, the magnetostructural phase transition takes place from a ferromagnetic high temperature phase to a low magnetization low temperature phase, therefore the magnetic and vibrational contributions to the total entropy change have a different sign, and the associated individual caloric effects are nonsynergic. Materials where both vibrational and magnetic contributions to the total entropy have the same sign are very appealing for multicaloric purposes because they are expected to exhibit synergic caloric effects [42]. Here we report on the multicaloric effect of a Ni-Mn-Ga-Cu alloy which undergoes a magnetostructural transition from a paramagnetic high temperature phase to a ferromagnetic low temperature phase which gives rise to synergic caloric effects.

In the prototype Ni_2MnGa magnetic shape memory alloy, it is known that substitution of Mn with Cu shifts the martensitic transition (MT) to higher temperatures while it decreases the Curie temperature [43]. The two transition lines joint at a triple point close to 6 at % Cu. As a result, the strength of the interplay between the structural and magnetic transitions increases as the amount of Cu increases and a magnetostructural transition from a paramagnetic high temperature parent phase to a ferromagnetic martensitic phase takes place above 6 at % Cu. Therefore, this material is expected to be a good candidate to show synergic magnetocaloric and elastocaloric effects. With this idea in mind, in the present work we have prepared a $\text{Ni}_{50}\text{Mn}_{18.5}\text{Ga}_{25}\text{Cu}_{6.5}$ alloy to study its multicaloric response under the combined application of uniaxial stress and magnetic field. A bespoke calorimeter that works under magnetic field and uniaxial stress has been employed to determine entropy changes as a function of temperature, magnetic field, and uniaxial stress. Based on these results, multicaloric as well as single caloric effects for the synergic-type $\text{Ni}_{50}\text{Mn}_{18.5}\text{Ga}_{25}\text{Cu}_{6.5}$ have been systematically investigated.

II. EXPERIMENT

An ingot with nominal composition $\text{Ni}_{50}\text{Mn}_{18.5}\text{Ga}_{25}\text{Cu}_{6.5}$ was prepared by arc-melting high-purity metals and then suction casted into a rodlike sample with a diameter of 7 mm in a copper mold. A crystallographically oriented polycrystalline rod was grown using the suction casted rod by the liquid-metal-cooling directional solidification method with a pulling rate of $150 \mu\text{m s}^{-1}$. Specimens with 3 mm diameter and 6 mm length were cut from the rod and were annealed at 1073 K for 24 h in an Ar atmosphere followed by quenching into a mixture of ice and water.

Calorimetric curves were measured using a bespoke calorimeter upon heating and cooling in a dual-field condition with applied magnetic fields up to $\mu_0 H = 6$ T, and applied uniaxial compressive stresses up to 20 MPa. The system is able to perform dilatometric measurements simultaneously. A detailed description of this system can be found in Ref. [44]. The transition entropy changes in the absence of applied magnetic field and applied uniaxial stress for both heating and cooling were determined from calorimetric curves obtained using a commercial DSC TA-Q2000.

Specific heat measurements of the sample at the martensitic and austenitic phases were performed using two different systems. On the one hand, a Physical Properties measurement system (PPMS, Quantum Design Inc.), operating in the relaxation method, was used to perform measurements within the temperature range from 330 to 400 K, under constant applied magnetic fields from 0 to 6 T (in 1 T steps). On the other hand, a Peltier cell calorimeter, described in detail in Refs. [45,46], was used to perform measurements within a temperature range from 50 to 350 K under constant applied magnetic fields from 0 to 3 T (in 1 T steps).

III. RESULTS AND DISCUSSION

Thermomagnetization curves (Fig. S1 in the Supplemental Material [47]) at selected values of magnetic field confirm the overlapping of martensite and magnetic transitions. The alloy undergoes a transition from a paramagnetic austenite to a ferromagnetic martensite.

Figures 1(a)–1(d) show the baseline corrected calorimetric curves obtained at selected values of magnetic field and under applied stresses of 0 and 20 MPa. The complete set of raw calorimetric curves is given in Fig. S2 (Supplemental Material [47]). Endothermic and exothermic peaks are observed upon heating and cooling, corresponding to the reverse and forward MT, respectively. Uniaxial stress and magnetic field shift the martensitic transition to higher temperatures due to the increase in stability of the ferromagnetic martensitic phase.

The forward and reverse transition temperatures can be identified by the temperature of the peak in the calorimetric curves recorded on cooling and heating, respectively. The magnetic field dependence of MT temperatures at constant values of the applied stress is shown in Fig. 1(e) and the stress dependence of the MT temperatures at constant values of the magnetic field is shown in Fig. 1(f). The complete phase diagram showing the transition temperatures in the H - σ space is given in Fig. S5(a) of the Supplemental Material [47]. It is

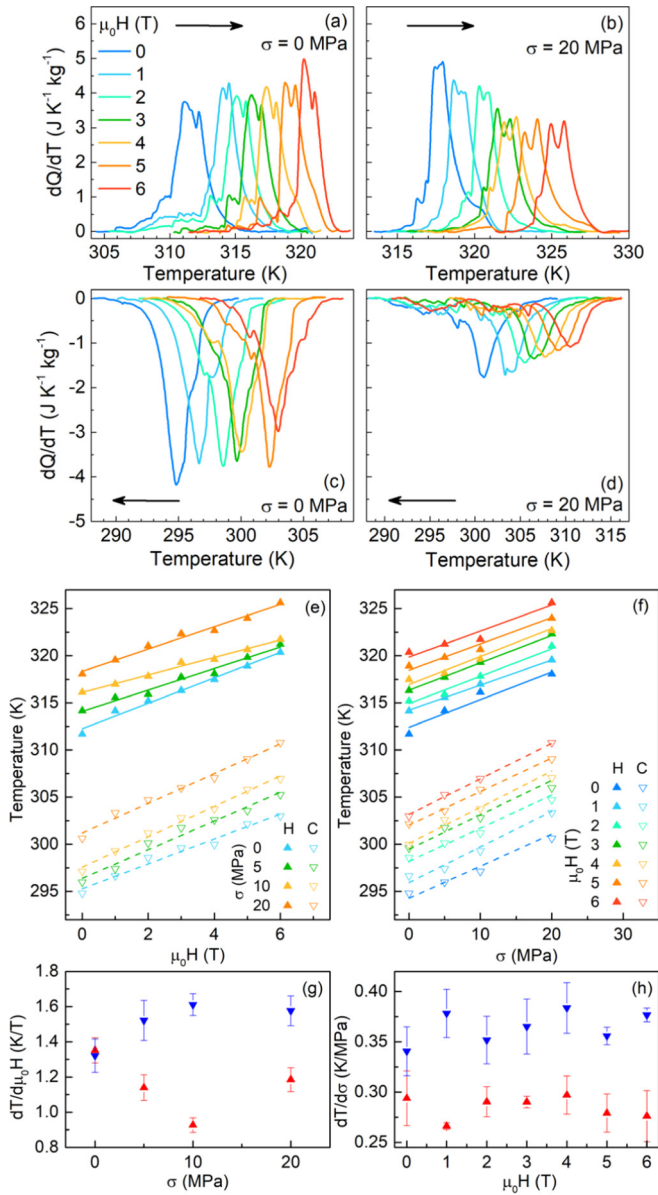


FIG. 1. Baseline corrected calorimetric curves at selected values of applied uniaxial stress and magnetic field for heating (a) and (b) and cooling (c) and (d) runs. Transition temperature as a function of magnetic field, for selected values of applied stress (e), and as a function of applied stress, for selected values of applied magnetic field (f). Open symbols correspond to the forward transition on cooling and solid symbols to the reverse transition on heating. Lines are the best fit to the data. (g) Stress dependence of the slope of transition temperature vs magnetic field lines. (h) Magnetic field dependence of the slope of the transition temperature vs stress lines.

apparent that, at constant stress, the MT temperatures linearly increase with increasing magnetic field, with slopes in the range 0.9 to 1.6 K T⁻¹. Furthermore, the value for the slope in the absence of applied stress ($\frac{dT}{\mu_0 dH} = 1.3 \pm 0.1$ K T⁻¹) is in good agreement with the value obtained in a previous study [29]. Application of uniaxial stress has little effect on the slope of the T vs H lines, and no clear tendency has been observed [Fig. 1(g)]. MT temperatures also increase with increasing uniaxial stress, with slope values in the range

$\frac{dT}{d\sigma} = 0.26$ to 0.38 K MPa⁻¹, with a weak dependence on magnetic field [Fig. 1(h)]. The synergic effect of magnetic field and uniaxial stress observed in Ni₅₀Mn_{18.5}Ga₂₅Cu_{6.5} where both magnetic field and stress shift the MT towards higher temperatures is in contrast to the behavior reported for metamagnetic shape memory alloys, such as Ni-Mn-In [33] and for Fe-Rh [37] in which magnetic field stabilizes the high temperature ferromagnetic phase thus shifting the magne-tostructural transition to lower temperatures.

The transition entropy change (ΔS_t) can be obtained from integration of the baseline corrected calorimetric curves (details are given in the Supplemental Material [47]), and results are shown in Fig. 2(a) where ΔS_t corresponding to forward and reverse MT are plotted as a function of magnetic field for selected values of uniaxial stress (a three-dimensional plot of ΔS_t vs H and σ is given in Fig. S5(b) of the Supplemental Material [47]). For all values of applied uniaxial stress, ΔS_t has been found to decrease with magnetic field, with slopes in the range -1.1 to -0.7 J kg⁻¹ K⁻¹ T⁻¹. For Ni₅₀Mn_{18.5}Ga₂₅Cu_{6.5} the vibrational and magnetic contributions to the transition entropy change have the same sign, and the expected increase of the magnetic contribution with increasing magnetic field cannot account for the observed decrease in the transition entropy change (in contrast to what happens in other metamagnetic shape memory alloys for which vibrational and magnetic contributions have a different sign [48]). The magnetic field dependence of ΔS_t found here may point to a certain interplay between the vibrational entropy and magnetic field. This hypothesis is supported by the enhanced softening at the Curie point of the low energy phonons in the TA₂ branch in composition related Ni-Mn-Ga alloys [49]. It is to be noticed that for metamagnetic shape memory alloys the vibrational contribution to the transition entropy change is magnetic field independent to a very good extent [48]. Further studies are required to clarify this issue, which is beyond the scope of the present work.

The combination of DSC calorimetric curves recorded under external applied fields and specific heat (C) data enables computation of caloric effects via the quasidirect method [9] (details for this computation are provided in the Supplementary Material [47]). While C can be considered as stress independent, for Ni₅₀Mn_{18.5}Ga₂₅Cu_{6.5}, as previously mentioned, phonons are sensitive to the applied magnetic field, and C is expected to be magnetic field dependent too. We have measured C at selected values of magnetic field, and results for $\mu_0 H = 0, 1, 2,$ and 3 T are shown in Fig. 2(b). It is apparent that application of magnetic field sharpens the calorimetric peak and shifts it to higher temperatures at an approximate rate of 1.4 K T⁻¹, which is in good agreement with the shift observed from the DSC measurements [see Fig. 1(e)]. The transition entropy values derived from the integration of these peaks decrease with increasing magnetic field at a rate ~ -0.5 J K⁻¹ kg⁻¹ T⁻¹, which is consistent with the data shown in Fig. 2(a). Additional specific heat measurements are given in Fig. S4 (Supplemental Material [47]).

Taking into account the magnetic field and temperature dependence of C and using the baseline corrected DSC calorimetric curves we have computed the entropy curves $S(T, \mu_0 H, \sigma)$, referenced to the the entropy value at $T_0 = 426$ K. The value of T_0 has been selected to be the temperature where the specific heat becomes magnetic field independent

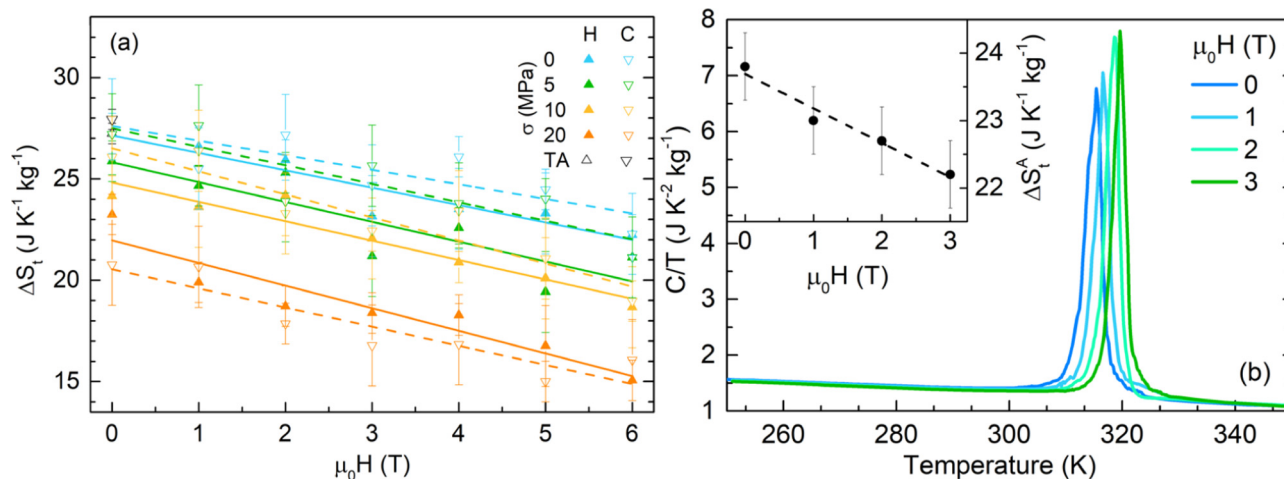


FIG. 2. (a) Magnetic field dependence of the transition entropy change at selected values of uniaxial stress. TA denotes the value at zero magnetic field and zero stress obtained using a commercial TA DSC. Open symbols correspond to the forward transition on cooling and solid symbols, to the reverse transition on heating. Lines are the best fit to the data. (b) Temperature dependence of the ratio between specific heat and temperature as a function of temperature for selected values of magnetic field. The inset shows the magnetic field dependence of the transition entropy change derived from the integration of the curves.

[see the Supplemental Material [47] Fig. S4(c)]. The temperature dependence of $S(T, \mu_0 H, \sigma)$ upon heating and cooling for selected values of magnetic field and uniaxial stress are shown in Fig. 3. In the low temperature region (in the martensitic phase) the increase in entropy with increasing magnetic field reflects the dependency of ΔS_t with magnetic field [see Fig. 2(a)].

As described in the Supplemental Material [47], the entropy curves enable computing single caloric (magnetocaloric

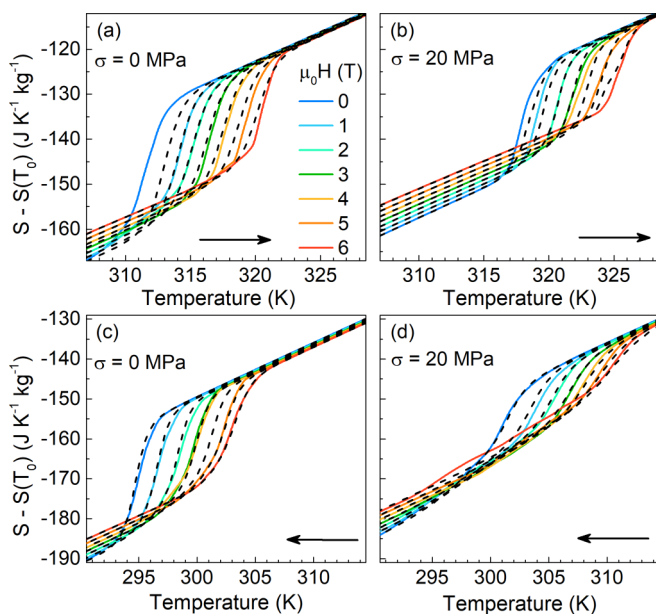


FIG. 3. Temperature dependence of the entropy upon heating (a) and (b) and cooling (c) and (d) runs at selected values of magnetic field and uniaxial stress. Solid curves correspond to the data from the integration of measured calorimetric curves and dashed lines correspond to the results from the fit. T_0 denotes the reference temperature ($T_0 = 426$ K).

and elastocaloric) effects. Results are given in the Supplemental Material [47] (Figs. S9–S12). As anticipated by the positive shift of the transition temperatures with uniaxial stress and magnetic field, both elastocaloric and magnetocaloric effects are conventional for $\text{Ni}_{50}\text{Mn}_{18.5}\text{Ga}_{25}\text{Cu}_{6.5}$.

Entropy curves $S(T, \mu_0 H, \sigma)$ computed from experimental data are only known for selected values of stress and magnetic field, and to obtain multicaloric effects over the entire $(T, \mu_0 H, \sigma)$ thermodynamic phase space it is necessary to define a numerical function to phenomenologically reproduce the behavior of the experimental isofield entropy curves over the entire phase space under study. Details of the fit are given in the Supplemental Material [47], and the results of the field for specific values of magnetic field and stress are compared in Fig. 3 to the curves directly computed from experimental data (additional curves are shown in Fig. S6, Supplemental Material [47]). A good agreement is observed between the two set of curves. Isofield and isothermal entropy surfaces are computed from the fitted entropy curves and illustrative examples for selected values of magnetic field, uniaxial stress and temperature are shown in Figs. S7 and S8 (Supplemental Material [47]).

The entropy and temperature changes associated with single caloric and multicaloric effects can readily be computed from the fitted $S(T, \mu_0 H, \sigma)$ functions as described in the Supplemental Material [47]. The values obtained for the elastocaloric and magnetocaloric effect (Figs. S13 and S14, Supplemental Material [47]) are in good agreement with those previously derived from the experimental curves. Such an agreement confirms the robustness of our fitting procedure and provides confidence in the multicaloric data derived from the fitted $S(T, \mu_0 H, \sigma)$.

In $\text{Ni}_{50}\text{Mn}_{18.5}\text{Ga}_{25}\text{Cu}_{6.5}$, both magnetic field and uniaxial stress favor the transition from austenite to martensite (as cooling does), and therefore the multicaloric effect resulting from application of magnetic field and uniaxial stress has to be computed from the entropy functions corresponding to

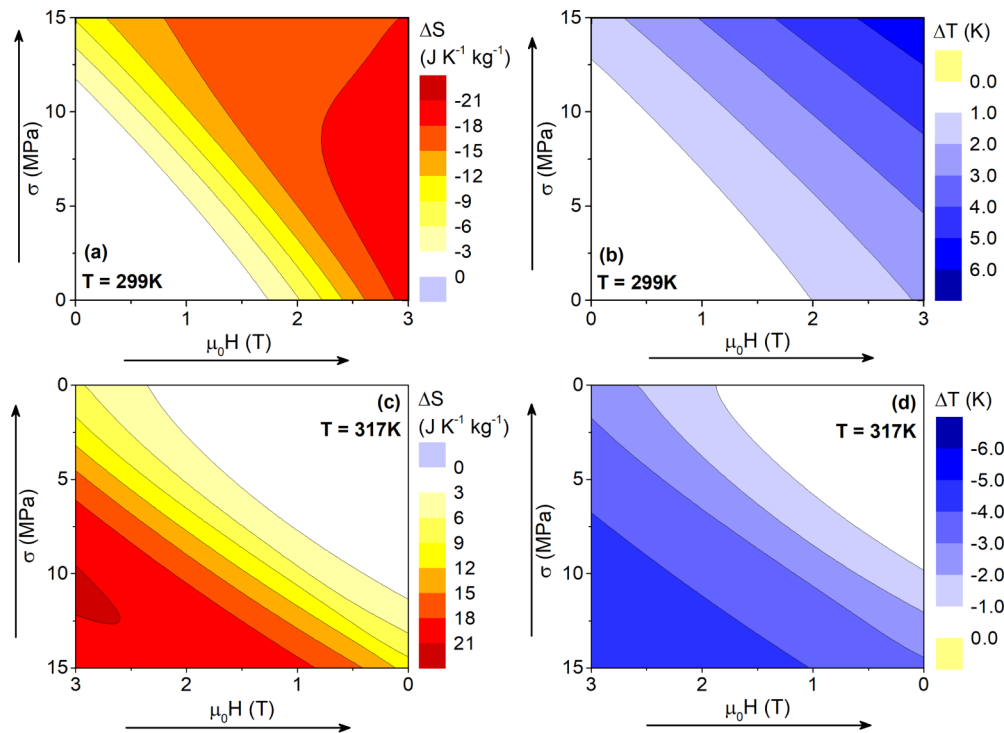


FIG. 4. Multicaloric isothermal entropy change (a) and adiabatic temperature change (b) resulting from the application of magnetic field and uniaxial stress at a temperature of 299 K. Multicaloric isothermal entropy change (c) and adiabatic temperature change (d) resulting from the removal of magnetic field and uniaxial stress at a temperature of 317 K.

cooling runs. On the other hand, the multicaloric effect resulting from the removal of magnetic field and uniaxial stress has to be computed from the entropy functions corresponding to heating runs. Illustrative results for the multicaloric ΔS and ΔT corresponding to the application of magnetic field and uniaxial stress at a temperature of 299 K are shown as color contour maps in Figs. 4(a) and 4(b), respectively. Illustrative results for the multicaloric ΔS and ΔT corresponding to the removal of magnetic field and uniaxial stress at a temperature of 317 K are shown in Figs. 4(c) and 4(d), respectively (additional data for a variety of temperatures around the transition region are shown in the Supplemental Material [47], Figs. S15 and S16).

When comparing ΔS and ΔT from single caloric effects to the values for the multicaloric effect, it is observed that significantly lower values of stress and magnetic field are required to obtain the same level of ΔS and ΔT when the two fields are combined. For instance, for the magnetocaloric effect at 299 K, a magnetic field of ~ 2.5 T is required to achieve $\Delta S = -14$ J kg⁻¹ K⁻¹, while when a uniaxial stress of 12 MPa is applied (multicaloric effect), the magnetic field needed to obtain the same value for ΔS is as low as 1 T. With regards to ΔT , a similar trend is observed. For instance, in the magnetocaloric case, for a temperature of 297 K, a magnetic field of 6 T gives rise to $\Delta T \sim 6.5$ K, while ΔT reaches 9.2 K when an additional stress of 20 MPa is applied in the multicaloric case. Such a synergic effect of dual fields also holds for the multicaloric response associated with removal of magnetic field and removal of uniaxial stress. A second remarkable outcome from the synergic response to

magnetic field and uniaxial stress is observed when comparing the maximum values for the adiabatic temperature change achieved in the multicaloric effect to those corresponding to single caloric effects: within the studied range of magnetic field and uniaxial stress, the value achieved under a dual field application ($\Delta T_{\max} > 9$ K), is larger than the largest values obtained for the magnetocaloric ($\Delta T_{\max} \sim 7$ K) and elastocaloric ($\Delta T_{\max} \sim 5$ K) effects. It is worth noticing that the contour color maps provide a guide to flexibly select combinations of magnetic field and stress to yield a tailored caloric response.

When considering the potential of multicaloric effects for future technological applications, it is particularly relevant to compare the field-induced multicaloric response under moderate magnetic fields (in the range of 1 T, which are readily accessible using permanent magnets), to the single magnetocaloric response in the same range of applied fields. The magnetocaloric adiabatic temperature change resulting from the application (or removal) of 1 T is in the range 0.9–1.7 K. However, the combination of the application (or removal) of a moderate stress with the application (or removal) of a magnetic field, results in significantly larger values: $\Delta T = 6.5$ K at $T = 296$ K (for the application of 20 MPa and 1 T), and $\Delta T = -5.4$ K at $T = 318$ K (for the removal of 20 MPa and 1 T).

In general, the multicaloric response of a given thermodynamic system is not obtained from the sum of single caloric effects because there is a contribution from a cross-coupling term [35] which accounts for the interplay between vibrational and magnetic degrees of freedom. While there is no

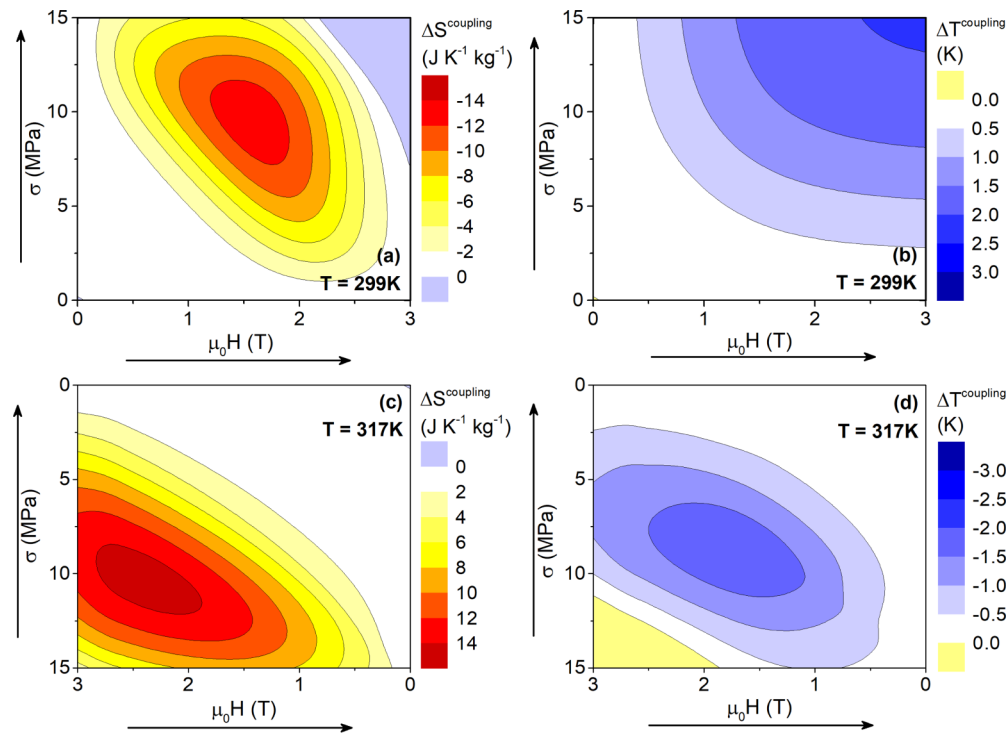


FIG. 5. Cross-coupling contribution to the multicaloric isothermal entropy (a) and (c) and adiabatic temperature (b) and (d) changes corresponding to the application of magnetic field and stress at $T = 299$ K (a) and (b), and to the removal of magnetic field and stress (c) and (d).

contribution from the cross-coupling term to the multicaloric response of materials with nonsynergic caloric effects [33], it becomes relevant in the multicaloric response when caloric effects are synergic. We have computed the contribution of the cross-coupling term to the total multicaloric entropy and temperature changes, as described in the Supplemental Material [47]. Illustrative results at 299 K (for the application of both magnetic field and uniaxial stress) and at 317 K (for the removal of both magnetic field and uniaxial stress) are shown in Fig. 5. It is found that the contribution from the cross-coupling term to the isothermal entropy and adiabatic temperature changes is weak for large values of the applied external fields (in the range where the phase transition is mostly induced by a single external field). However, this term becomes relevant at low external fields, and it is responsible for the increase in ΔS and ΔT values when compared to single caloric effects. In addition, the cross-coupling contribution is responsible for the broadening of the range of fields (stress and magnetic field) where giant caloric effects are observed.

It is worth mentioning that the cross-coupling contribution for the removal (application) of the external fields is only relevant within a certain temperature window. When the temperature (T) is slightly higher than the transition temperature in the absence of external fields ($T \gtrsim T_i$), the cross-coupling contribution is not relevant because removal (application) of a single stimulus (magnetic field or stress) suffices to induce the martensitic transition. Conversely, at higher temperatures that are further away from the transition temperature in the absence of external fields ($T > T_i$), the cross-coupling contribution becomes significant for both processes and enhances the multicaloric response of the material.

IV. SUMMARY AND CONCLUSIONS

We have studied the multicaloric response of $\text{Ni}_{50}\text{Mn}_{18.5}\text{Ga}_{25}\text{Cu}_{6.5}$ subjected to the combined action of magnetic field and uniaxial stress, for which elastocaloric and magnetocaloric effects are conventional and act in a synergic manner. A proper numerical treatment of the calorimetric curves measured under selected values of magnetic field and uniaxial stress has enabled us to compute the entropy $S(T, \mu_0 H, \sigma)$ over the entire phase space within the studied field ranges (20 MPa and 6 T). We have computed the multicaloric isothermal entropy change and adiabatic temperature change for any combination of application and removal of magnetic field and stress, and we have also evidenced the contribution of the interplay between magnetic and vibrational degrees of freedom to these quantities. We have shown that the combined action of magnetic field and uniaxial stress increases the reversibility of caloric effects. It has also been shown that the maximum adiabatic temperature change that results from the multicaloric effect (above 9 K) is larger than the maximum value that can be achieved for a single caloric effect. Furthermore, the magnitude of the field needed to obtain a certain value for ΔS or ΔT is significantly lowered when a second field is applied, and it has been shown that such a reduction is predominantly due to the contribution of the cross coupling between magnetism and structure. Another advantage brought by dual-field application is the expansion of the temperature window where giant caloric effects occur, when compared to that corresponding to single caloric effects.

Present results are expected to be extrapolable to other multicaloric materials with synergic individual caloric effects, and therefore our work provides guidelines in designing

multicaloric cooling devices using materials with synergistic caloric effects.

Raw and processed data are available on request from the authors.

ACKNOWLEDGMENTS

Financial support from the MCIN/AEI/10.13039/501100011033 (Spain) under Grant No. PID2020-

113549RB-I00/AEI/ and from the International Partnership Program of Chinese Academy of Sciences (Grant No.174433KYSB20180040) are acknowledged. A.G.-C. acknowledges financial support from the Universitat de Barcelona under the APIF scholarship. Z.W. and J.L. acknowledge Zhejiang Provincial Natural Science Foundation of China (Grants No. LD21E010001 and No. 51801225). We acknowledge F. Guillou and H. Yibole for experimental support.

- [1] W. Goetzler, R. Zogg, J. Young, and C. Johnson, *Energy Savings Potential and RD&D Opportunities for Nonvapor-Compression HVAC Technologies* (U.S. Department of Energy, Burlington, 2014).
- [2] V. K. Pecharsky and K. A. Gschneidner Jr., Giant Magnetocaloric Effect in $Gd_5(Si_2Ge_2)$, *Phys. Rev. Lett.* **78**, 4494 (1997).
- [3] A. S. Mischenko, Q. Zhang, J. F. Scott, and N. D. Mathur, Giant electrocaloric effect in thin-film $PbZr_{0.95}Ti_{0.05}O_3$, *Science* **311**, 1270 (2006).
- [4] E. Bonnot, R. Romero, L. Mañosa, E. Vives, and A. Planes, Elastocaloric Effect Associated with the Martensitic Transition in Shape-Memory Alloys, *Phys. Rev. Lett.* **100**, 125901 (2008).
- [5] B. F. Lu, F. Xiao, A. R. Yan, and J. Liu, Elastocaloric effect in a textured polycrystalline Ni-Mn-In-Co metamagnetic shape memory alloy, *Appl. Phys. Lett.* **105**, 161905 (2014).
- [6] L. Mañosa, D. Gonzalez-Alonso, A. Planes, E. Bonnot, M. Barrio, J. L. Tamarit, S. Aksoy, and M. Acet, Giant solid-state barocaloric effect in the Ni-Mn-In magnetic shape-memory alloy, *Nat. Mater.* **9**, 478 (2010).
- [7] X. Moya, S. Kar-Narayan, and N. D. Mathur, Caloric materials near ferroic phase transitions, *Nat. Mater.* **13**, 439 (2014).
- [8] V. Franco, J. S. Blázquez, B. Ingale, and A. Conde, The magnetocaloric effect and magnetic refrigeration near room temperature: Materials and models, *Annu. Rev. Mater. Res.* **42**, 305 (2012).
- [9] L. Mañosa and A. Planes, Materials with giant mechanocaloric effects: Cooling by strength, *Adv. Mater.* **29**, 1603607 (2017).
- [10] T. Gottschall, K. P. Skokov, M. Fries, A. Taubel, I. Radulov, F. Scheibel, D. Benke, S. Riegg, and O. Gutfleisch, Making a cool choice: The materials library of magnetic refrigeration, *Adv. Energy Mater.* **9**, 1901322 (2019).
- [11] Y. Liu, J. F. Scott, and B. Dkhil, Direct and indirect measurements on electrocaloric effect: Recent developments and perspectives, *Appl. Phys. Rev.* **3**, 031102 (2016).
- [12] B. Li, Y. Kawakita, S. Ohira-Kawamura, T. Sugahara, H. Wang, J. Wang, Y. Chen, S. I. Kawaguchi, S. Kawaguchi, K. Ohara *et al.*, Colossal barocaloric effects in plastic crystals, *Nature (London)* **567**, 506 (2019).
- [13] A. Aznar, P. Lloveras, M. Barrio, Ph. Negrier, A. Planes, L. Mañosa, N. D. Mathur, X. Moya, and J. L. Tamarit, Reversible and irreversible colossal barocaloric effects in plastic crystals, *J. Mater. Chem. A* **8**, 639 (2020).
- [14] P. Lloveras, A. Aznar, M. Barrio, Ph. Negrier, C. Popescu, A. Planes, L. Mañosa, E. Stern-Taulats, A. Avramenko, N. D. Mathur, X. Moya, and J. Ll. Tamarit, Colossal barocaloric effects near room temperature in plastic crystals of neopentylglycol, *Nat. Commun.* **10**, 1803 (2019).
- [15] S. P. Vallone, A. N. Tantillo, A. M Dos Santos, J. J. Molaison, R. Kulmaczewski, A. Chapoy, P. Ahmadi, M. A. Halcrow, and K. G. Sandeman, Giant barocaloric effect at the spin crossover transition of a molecular crystal, *Adv. Mater.* **31**, 1807334 (2019).
- [16] M. Romanini, Y. X. Wang, K. Gurbinar, G. Ornelas, P. Lloveras, Y. Zhang, W. Zheng, M. Barrio, A. Aznar, A. Gràcia-Condal *et al.*, Giant and reversible barocaloric effect in trinuclear spin-crossover complex $Fe_3(bntrz)_6(tenset)_6$, *Adv. Mater.* **33**, 2008076 (2021).
- [17] Z. Y. Wei, E. K. Liu, J. H. Chen, Y. Li, G. D. Liu, H. Z. Luo, X. K. Xi, H. W. Zhang, W. H. Wang, and G. H. Wu, Realization of multifunctional shape-memory ferromagnets in all-*d*-metal Heusler phases, *Appl. Phys. Lett.* **107**, 022406 (2015).
- [18] Z. Y. Wei, E. K. Liu, Y. Li, X. L. Han, Z. W. Du, H. Z. Luo, G. D. Liu, X. K. Xi, H. W. Zhang, W. H. Wang, and G. H. Wu, Magnetostructural martensitic transformations with large volume changes and magneto-strains in all-*d*-metal Heusler alloys, *Appl. Phys. Lett.* **109**, 071904 (2016).
- [19] E. K. Liu, Z. Y. Wei, W. H. Wang, X. Xi, J. Chen, and G. Wu, US Patent, US10279391B2. 2019.
- [20] A. Aznar, A. Gràcia-Condal, A. Planes, P. Lloveras, M. Barrio, J. L. Tamarit, W. Xiong, D. Cong, C. Popescu, and L. Mañosa, Giant barocaloric effect in all-*d*-metal Heusler shape memory alloys, *Phys. Rev. Materials* **3**, 044406 (2019).
- [21] Z. Y. Wei, Y. Shen, Z. Zhang, J. Guo, B. Li, E. Liu, Z. Zhang, and J. Liu, Low-pressure-induced giant barocaloric effect in an all-*d*-metal Heusler $Ni_{35.5}Co_{14.5}Mn_{35}Ti_{15}$ magnetic shape memory alloy, *APL Mater.* **8**, 051101 (2020).
- [22] Z. Y. Wei, W. Sun, Q. Shen, Y. Shen, Y. F. Zhang, E. K. Liu, and J. Liu, Elastocaloric effect of all-*d*-metal Heusler NiMnTi(Co) magnetic shape memory alloys by digital image correlation and infrared thermography, *Appl. Phys. Lett.* **114**, 101903 (2019).
- [23] D. Cong, W. Xiong, A. Planes, Y. Ren, L. Mañosa, P. Cao, Z. Nie, X. Sun, Z. Yang, X. Hong, and Y. Wang, Colossal Elastocaloric Effect in Ferroelastic Ni-Mn-Ti Alloys, *Phys. Rev. Lett.* **122**, 255703 (2019).
- [24] H. L. Yan, L. D. Wang, H. X. Liu, X. M. Huang, N. Jia, Z. B. Li, B. Yang, Y. D. Zhang, C. Esling, X. Zhao, and L. Zuo, Giant elastocaloric effect and exceptional mechanical properties in an all-*d*-metal Ni-Mn-Ti alloy: Experimental and ab-initio studies, *Mater. Design* **184**, 108180 (2019).
- [25] O. Gutfleisch, T. Gottschall, M. Fries, D. Benke, I. Radulov, K. P. Skokov, H. Wende, M. Gruner, M. Acet, P. Entel, and M.

- Farle, Mastering hysteresis in magnetocaloric materials, *Philos. Trans. R. Soc. London Ser. A* **374**, 20150308 (2016).
- [26] A. Kitanovski, Energy applications of magnetocaloric materials, *Adv. Energy Mater.* **10**, 1903741 (2020).
- [27] S. X. Qian, D. Nasuta, A. Rhoads, Y. Wang, Y. Geng, Y. Hwang, R. Radermacher, and I. Takeuchi, Not-in-kind cooling technologies: A quantitative comparison of refrigerants and system performance, *Int. J. Refrig.* **62**, 177 (2016).
- [28] Y. Song, X. Chen, V. Dabade, T. W. Sheld, and R. D. James, Enhanced reversibility and unusual microstructure of a phase-transforming material, *Nature (London)* **502**, 85 (2013).
- [29] D. Zhao, J. Liu, X. Chen, W. Sun, Y. Li, M. Zhang, Y. Shao, H. Zhang, and A. Yan, Giant caloric effect of low-hysteresis metamagnetic shape memory alloys with exceptional cyclic functionality, *Acta Mater.* **133**, 217 (2017).
- [30] C. Chluba, W. Ge, R. L. De Miranda, J. Strobel, L. Kienle, E. Quandt, and M. Wuttig, Ultralow-fatigue shape memory alloy films, *Science* **348**, 1004 (2015).
- [31] H. Hou, P. Finkel, M. Staruch, J. Cui, and I. Takeuchi, Ultra-low-field magneto-elastocaloric cooling in a multiferroic composite device, *Nat. Commun.* **9**, 4075 (2018).
- [32] J. Liu, T. Gottschall, K. P. Skokov, J. D. Moore, and O. Gutfleisch, Giant magnetocaloric effect driven by structural transitions, *Nat. Mater.* **11**, 620 (2012).
- [33] A. Gràcia-Condal, T. Gottschall, L. Pfeuffer, O. Gutfleisch, A. Planes, and L. Mañosa, Multicaloric effects in metamagnetic Heusler Ni-Mn-In under uniaxial stress and magnetic field, *Appl. Phys. Rev.* **7**, 041406 (2020).
- [34] E. Stern-Taulats, T. Castán, L. Mañosa, A. Planes, N. D. Mathur, and X. Moya, Multicaloric materials and effects, *MRS Bull.* **43**, 295 (2018).
- [35] A. Planes, T. Castan, and A. Saxena, Thermodynamics of multicaloric effects in multiferroic materials: Application to metamagnetic shape-memory alloys and ferrotoroidics, *Philos. Trans. R. Soc. London Ser. A* **374**, 20150304 (2016).
- [36] P. O. Castillo-Villa, D. E. Soto-Parra, J. A. Matutes-Aquino, R. A. Ochoa-Gamboa, A. Planes, L. Mañosa, D. Gonzalez-Alonso, M. Stipcich, R. Romero, D. Rios-Jara, and H. Flores-Zuñiga, Caloric effects induced by magnetic and mechanical fields in a $\text{Ni}_{50}\text{Mn}_{25-x}\text{Ga}_{25}\text{Co}_x$ magnetic shape memory alloy, *Phys. Rev. B* **83**, 174109 (2011).
- [37] E. Stern-Taulats, T. Castán, A. Planes, L. H. Lewis, R. Barua, S. Pramanick, S. Majumdar, and L. Mañosa, Giant multicaloric response of bulk $\text{Fe}_{49}\text{Rh}_{51}$, *Phys. Rev. B* **95**, 104424 (2017).
- [38] A. Czernuszewicz, J. Kaleta, and D. Lewandowski, Multicaloric effect: Toward a breakthrough in cooling technology, *Energy Convers. Manage.* **178**, 335 (2018).
- [39] A. Gràcia-Condal, E. Stern-Taulats, A. Planes, and L. Mañosa, Caloric response of $\text{Fe}_{49}\text{Rh}_{51}$ subjected to uniaxial load and magnetic field, *Phys. Rev. Materials* **2**, 084413 (2018).
- [40] H. Hou, S. Qian, and I. Takeuchi, Materials, physics and systems for multicaloric cooling, *Nat. Rev. Mater.* (2022), doi: 10.1038/s41578-022-00428-x
- [41] F. X. Liang, J. Z. Hao, F. R. Shen, H. B. Zhou, J. Wang, F. X. Hu, J. He, J. R. Sun, and B. G. Shen, Experimental study on coupled caloric effect driven by dual fields in metamagnetic Heusler alloy $\text{Ni}_{50}\text{Mn}_{35}\text{In}_{15}$, *APL Mater.* **7**, 051102 (2019).
- [42] H. Qian, J. Guo, Z. Wei, and J. Liu, Multicaloric effect in synergic magnetostructural phase transformation Ni-Mn-Ga-In alloys, *Phys. Rev. Materials* **6**, 054401 (2022).
- [43] D. W. Zhao, T. Castán, A. Planes, Z. Li, W. Sun, and J. Liu, Enhanced caloric effect induced by magnetoelastic coupling in NiMnGaCu Heusler alloys: Experimental study and theoretical analysis, *Phys. Rev. B* **96**, 224105 (2017).
- [44] A. Gràcia-Condal, E. Stern-Taulats, A. Planes, E. Vives, and L. Mañosa, The giant elastocaloric effect in a Cu-Zn-Al shape-memory alloy: A calorimetric study, *Phys. Status Solidi (b)* **255**, 1700422 (2018).
- [45] G. Porcari, F. Cugini, S. Fabbri, C. Pernechele, F. Albertini, M. Buzzi, M. Mangia, and M. Solzi, Convergence of direct and indirect methods in the magnetocaloric study of first order transformations: The case of Ni-Co-Mn-Ga Heusler alloys, *Phys. Rev. B* **86**, 104432 (2012).
- [46] F. Guillou, G. Porcari, H. Yibole, N. van Dijk, and E. Bruck, Taming the first-order transition in giant magnetocaloric materials, *Adv. Mater.* **26**, 2671 (2014).
- [47] See Supplemental Material at <http://link.aps.org/supplemental/10.1103/PhysRevMaterials.6.084403> for additional experimental and analytical details.
- [48] T. Gottschall, K. P. Skokov, D. Benke, M. Gruner, and O. Gutfleisch, Contradictory role of the magnetic contribution in inverse magnetocaloric Heusler materials, *Phys. Rev. B* **93**, 184431 (2016).
- [49] M. Acet, L. Mañosa, and A. Planes, Magnetic-field-induced effects in martensitic Heusler-based magnetic shape memory alloys, *Handbook Magn. Mater.* **19**, 231 (2011).